Advantages of a Topographically Controlled Runoff Simulation in a Soil–Vegetation–Atmosphere Transfer Model

Article *in* Journal of Hydrometeorology · April 2002

DOI: 10.1175/1525-7541(2002)003<0131:AOATCR>2.0.CO;2

CITATIONS
74

READS
83

4 authors, including:

Kirsten Warrach-Sagi
University of Hohenheim
107 PUBLICATIONS **4,494** CITATIONS

SEE PROFILE

Heinz-Theo Mengelkamp
anemos GmbH
57 PUBLICATIONS **664** CITATIONS

SEE PROFILE

Advantages of a Topographically Controlled Runoff Simulation in a Soil–Vegetation–Atmosphere Transfer Model

KIRSTEN WARRACH*

Institute of Atmospheric Physics, GKSS Research Center, Geesthacht, Germany

MARC STIEGLITZ

Lamont-Doherty Earth Observatory, Palisades, New York

HEINZ-THEO MENGELKAMP AND EHRHARD RASCHKE

GKSS Research Center, Institute of Coastal Research, Geesthacht, Germany

(Manuscript received 23 February 2001, in final form 4 September 2001)

ABSTRACT

Two methods to incorporate subgrid variability in soil moisture and runoff production into soil–vegetation–atmosphere transfer (SVAT) models are compared: 1) the variable infiltration capacity model approach (VIC), and 2) a modified ''TOPMODEL'' approach. Because neither approach needs to track surface or subsurface flow within a catchment explicitly, they represent computationally efficient ways to represent hydrologic processes within the context of regional and global modeling. This study shows that, during low flow periods, the runoff simulation is superior when using the TOPMODEL-based equations, especially during the rising limb of the autumn hydrograph. A main drawback of the modified VIC-model approach, especially for regional and global application, is that, with five free parameters, considerably more model calibration is required. TOPMODEL, on the other hand, requires only the determination of one free parameter. However, a TOPMODEL approach does require extensive preprocessing of topographic data, and issues concerning resolution of the data used become relevant.

1. Introduction

The term land surface model (LSM) typically has been used in the context of global and regional climate modeling. LSMs serve as the lower boundary to atmospheric general circulation models (GCMs). Standard LSMs employ a one-dimensional (vertical) treatment of subsurface moisture transport and surface moisture and energy fluxes that effectively assumes homogeneous soil moisture conditions across horizontal areas spanning hundreds of kilometers. The complexity of these models ranges from simple bucket models to sophisticated soil–vegetation–atmosphere transfer (SVAT) schemes with multiple vegetation, soil, and snow layers (e.g., Koster et al. 2000; Slater et al. 2001). The water and energy fluxes between the land surface and the atmosphere are linked via the evapotranspiration and latent heat flux, respectively. The LSM partitions the precipitation into evapotranspiration, runoff, and soil moisture change and the net incoming radiation into a latent and sensible heat flux, ground heat flux, and snowmelt energy. Most SVAT (e.g., Verseghy et al. 1993; Noilhan and Planton 1989; Yang and Dickinson 1996) studies (e.g., Chen et al. 1996; Schulz et al. 1998) focus on determining the energy fluxes. However, the calculation of runoff and the calculation of evapotranspiration are strongly related. A poor runoff calculation results in an unrealistic latent heat flux, regardless of which scheme is used (Koster et al. 2000). The Project for Intercomparison of Land Surface Parameterization Schemes (PILPS; Henderson-Sellers et al. 1993) has focused attention on the runoff calculation by SVAT models (e.g., Wood et al. 1998; Habets et al. 1999; Koster et al. 2000). The recent Global Energy and Water Cycle Experiment project has placed emphasis explicitly on improving the representation of both the horizontal and vertical water fluxes in LSMs as applied to GCMs. Further, as large-scale weather and climate model applications diversify to water-related issues such as water resources, reservoir management, and flood and drought forecasting, attention is beginning to focus on the purely hydrologic aspects

* Current affiliation: Max-Planck-Institut für Meteorologie, Hamburg, Germany.

Corresponding author address: Kirsten Warrach, Max Planck Institute for Meteorology, Bundesstr. 55, 20146 Hamburg, Germany.
E-mail: warrach@dkrz.de

of these LSMs. Graham and Bergström (2000) give an overview of the differences of land surface modeling in regional hydrology and meteorology as well as the requirements and advantages of combining the disciplines for investigations of the energy and water fluxes.

A critical deficiency in standard GCM-based LSMs is the neglect of an explicit treatment for spatial variability in soil moisture. Development work by various groups has focused on improving the 1D representation itself, incorporating, for example, more physiologically based vegetation schemes so as to determine transpiration and canopy–atmosphere CO_2 fluxes better (Sellers et al. 1986; Bonan 1995; Kucharik et al. 2000), but relatively little attention has been given to the spatial heterogeneity issue concerning soil moisture and resulting runoff production. This lack of attention is unfortunate, given that this heterogeneity can have a strong impact on surface energy and water budgets. However, there has been substantial recent progress with respect to modeling control of the catchment's characteristics such as topography and spatial soil distribution over surface hydrologic processes. Two approaches to improving simulated runoff in LSMs have become especially popular.

1) A variable infiltration capacity model approach, or VIC, indirectly accounts for the impact that topography and soil distribution have on surface infiltration (Dümenil and Todini 1992; Wood et al. 1992; Liang et al. 1994). As opposed to the definition employed by soil physicists, ''infiltration capacity'' here is defined as the total volumetric capacity of a soil column to hold water. This concept does not necessarily need topographic data; the parameters can be calibrated to the catchment. However, within hilly and mountainous catchments, the topography determines the distribution of soil type, soil depth, and water table. When calibrating the parameters for the VIC approach, the indirect effect of topography on the hydrological behavior is represented. In addition, for areas characterized by steep slopes, Dümenil and Todini (1992) used the topographical variability to determine the parameters. A recent study by S. Hagemann from the Max Planck Institute for Meteorology in Germany (2001, personal communication) underscores the correlation of topography and VIC parameters. Apart from its application in macroscale hydrologic modeling (e.g., Liang et al. 1996; Nijssen et al. 2001), the VIC formulation has been used with the European Climate Model-Hamburg Version (ECHAM) LSM (Dümenil and Todini 1992; Hagemann and Dümenil 1999) and the Interactions between Soil, Biosphere, and Atmosphere (ISBA) LSM (Habets et al. 1999).
2) Another approach, ''TOPMODEL'' (Beven and Kirkby 1979), uses topographic information to determine the statistical distribution of the catchment's water table depth and the impact this heterogeneity has on runoff generation. Another feature of this approach is the formulation of a vertical depth-dependent effective saturated hydraulic conductivity, whose exponential decay factor can be calibrated. The distinction between the saturated and unsaturated fraction of the catchment is also accounted for in the calculation of the evapotranspiration, whereas in the VIC model this is only done for the evaporation from bare soil. Application of TOPMODEL formulations with typical SVAT schemes have been conducted by numerous groups (Famiglietti and Wood 1994; Stieglitz et al. 1997; Ducharne et al. 2000) on the local and regional scale.

Both VIC-model and TOPMODEL approaches can be applied at regional scales (Famiglietti and Wood 1994; Liang et al. 1994; Ducharne et al. 2000; Koster et al. 2000) and therefore are suitable for LSMs to be used with mesoscale and regional GCMs.

More than 20 LSMs participated in the ongoing PILPS intercomparison experiments (e.g., Chen et al. 1997; Wood et al. 1998; Slater et al. 2001). One such model, Surface Energy and Water Balance (SEWAB; Mengelkamp et al. 1999), is a one-dimensional SVAT scheme solving the coupled surface energy and water balance equations and the vertical heat and water fluxes within the soil column. In its original formulation, SEWAB only calculated runoff as free drainage from its lowest modeled soil layer, and as infiltration and saturation excess runoff. The advantage of such a simple and common approach is that no calibration of free runoff parameters is necessary [soil and vegetation parameters are taken from published lookup tables such as in Rawls et al. (1993)]. The disadvantage is that this scheme often yields a poor runoff simulation because of too little surface and too fast subsurface response.

As with most LSMs, SEWAB was developed primarily for applications with an atmospheric model and therefore differs from those developed for purely hydrologic modeling (i.e., VIC and TOPMODEL). In this study, we incorporate the hydrologic formulations of VIC and TOPMODEL with the land–atmosphere formulations of SEWAB and demonstrate the benefits of doing so. Using an 8.4 km^2 watershed in the northeastern United States, we demonstrate the advantages and disadvantages of employing the runoff formulations 1) of the VIC-3L model (see appendix A) with SEWAB; 2) of TOPMODEL (see appendix B) with SEWAB; and 3), for completeness, of the original SEWAB approach.

2. Description of SEWAB

The one-dimensional (vertical) land surface model SEWAB (Mengelkamp et al. 1999; Warrach et al. 2001) is designed to be coupled to atmospheric models or run

offline with forcing data. It calculates the vertical water and energy fluxes between the land surface and the atmosphere and within the soil column for a land surface grid cell. A land surface grid cell typically has horizontal dimensions of 1–100 km.

In SEWAB, both water and energy balance equations are solved at the land surface interface. The surface energy balance equation describes the equilibrium of net irradiance, latent heat flux, sensible heat flux, and soil heat flux (and, in the case of snow, the energy available for melting). Precipitation is partitioned into runoff, evapotranspiration, and change of snowpack and soil moisture storage. The evapotranspiration is calculated separately for bare soil and vegetated parts of the land surface grid cell by following the approach of Noilhan and Planton (1989).

Warrach et al. (2001) incorporated a single-layer snow model to allow for a partially snow-covered land surface grid cell. This snow model solves the energy balance for a snowpack and accounts for changes in density and surface albedo due to snowpack aging. Snowpack meltwater either infiltrates into the soil or leaves the land surface as runoff.

The soil column is divided into a variable number of model layers; at least four are recommended to allow a higher vertical resolution within the root zone. Within the soil column, temperature diffusion (with a term for soil freezing) and the Richards equation are solved with a semi-implicit Thomas algorithm by Richtmyer and Morton (1967) to avoid the excessively small time steps made necessary by the very thin uppermost layer. The Richards equation is modified to allow for root water uptake and soil freezing. The temperature of the first model layer is solved from the surface energy balance. The lower boundary temperature is prescribed by a time series representing the annual cycle. Leaf drip, precipitation on bare soil, evaporation from bare soil, and the soil moisture are accounted for. Surface runoff is generated when the infiltration capacity is exceeded. The lower boundary condition is given by free drainage. In SEWAB's standard version, water draining into a saturated compartment or reaching the lower boundary depth immediately generates subsurface runoff.

3. Modifications of the runoff simulation

Horizontal variability of runoff processes and the spatial distribution of the soil moisture are not explicitly described in a one-dimensional vertical LSM. Two approaches to incorporate subgrid variability in soil moisture and runoff production into SVAT models have become popular: 1) the Xinanjiang or Arno or VIC model and 2) a modified TOPMODEL approach. Both concepts originate from rainfall–runoff models and can be used with typical SVAT schemes in a computationally efficient way. See appendices A and B for a detailed description of the VIC-model and TOPMODEL runoff calculations.

Both the VIC model and TOPMODEL attempt to maintain a distributed description of catchment responses but in an empirical (VIC model) or statistical (TOPMODEL) manner, without the need to represent hillslope processes explicitly (Beven 2000). The VIC model uses a simple functional form to represent the spatial variability of runoff generation processes. The attraction of the VIC model is that it provides a method to determine subgrid soil moisture, and therefore evapotranspiration and runoff, without the need to resort to any topographic data whatsoever. However, the cost of not using any topographic data to determine the hillslope control over hydrologic processes is that five model parameters need to be determined, presumably from calibration with discharge data. There are six (five in case the total soil depth is given) parameters that require calibration. The VIC model performs increasingly well with increasing gridcell size, as can be seen from applications by Liang et al. (1994) at the local scale, by Lohmann et al. (1998c) at the regional scale, and by Abdulla et al. (1996) at the global scale. However, for applications with GCM SVATs, it is clearly advantageous to have as few adjustable parameters as possible.

The attraction of the TOPMODEL approach is that it is derived from first principles, makes use of site-specific topographic data, and, in theory, requires only one calibration parameter, the vertical profile of the effective saturated hydraulic conductivity. Various authors (e.g., Sivapalan et al. 1987; Famiglietti and Wood 1994) outlined ways to incorporate the TOPMODEL framework (Beven and Kirkby 1979) into LSMs. Based on their work, Stieglitz et al. (1997) introduced a concept to include the analytical TOPMODEL equations into an SVAT model in a computationally efficient way. Koster et al. (2000) present a catchment-based LSM for GCMs that uses the TOPMODEL framework. These modified TOPMODEL approaches utilize the distribution of the topography within a catchment to account for the spatial distribution of water-table depth and the resulting runoff production. However, it is still an open question as to what resolution of digital elevation model (DEM) is required to represent hillslope processes accurately (e.g., Zhang and Montgomery 1994; Wolock and McCabe 2000). Further, the TOPMODEL approach is limited to gridcell sizes of several kilometers by the assumption that the groundwater table is recharged at a spatially uniform and steady rate with respect to the response timescale of the watershed. However, even at larger spatial scales, Koster et al. (2000) state, supported by applications of Ducharne et al. (2000), that TOPMODEL ''nevertheless captures the critical differences between upslope and downslope hydrological behavior and should give a useful first-order description of subgrid soil moisture variability.''

The SVAT model SEWAB has the option to use the

runoff formulation of either the VIC model or the TOPMODEL approach. In contrast with the original VIC model, SEWAB has a variable number of soil layers with a minimum of three layers. This implies that the variable infiltration capacity (and resulting direct runoff) calculation is based on the root zone while base flow as in the VIC model is calculated from the deepest soil layer (e.g., Nijssen et al. 2001).

4. Application to the Sleepers River watershed

a. Site description

The Sleepers River watershed (111 km^2) located in the glaciated highlands of Vermont is hydrologically representative of most upland regions in the northeastern United States. As such, this site was chosen in 1957 as an experimental watershed by the Agricultural Research Service (ARS) to provide a better understanding of natural watershed behavior and to aid in the development of testing physically based hydrologic models (Anderson 1976). Nested entirely within the Sleepers River watershed is the W3 subwatershed (8.4 km^2). The topography is characterized by rolling hills, and the soils are predominantly silty loams. Vegetation cover is approximately equally distributed among grasses, coniferous forest, and deciduous forest. It is the 5 yr of meteorological and hydrologic data collected in this watershed between 1969 and 1974 that are used to drive and to evaluate our LSM schemes. Hourly measurements of air temperature, dewpoint temperature, incoming shortwave and thermal radiation, and wind speed were taken. The mean hourly precipitation is determined from seven gauges placed within the W3 subcatchment. Another dataset contains the snow water equivalent (Fig. 1), snow depth, snow temperature, and soil temperature. Hourly runoff data are available from a gauge at which the Pope Brook leaves the W3 subcatchment of the Sleepers River.

For the period 1970–74 the annual mean precipitation is 1250 mm and discharge is 730 mm for the W3 subcatchment of the Sleepers River. The precipitation is evenly distributed throughout the year (Fig. 2), with precipitation occurring on 50% of the days. Of the daily precipitation, 10% is less than 1 mm and 40% is between 1 and 10 mm. In summer and autumn, the catchment's runoff/precipitation is between 10% and 20%. The annual cycle of the measured discharge is characterized by low flow (about 0.5–1 mm day^{-1}) from about June until March and by high flow (maximum between 11 and 24 mm day^{-1}) due to snowmelt from about March to June. There is an immediate response of the catchment's discharge to rainfall events that can be seen in strong, almost spiky peaks in the measurements (Figs. 3–7, gray line). In 1972 and 1973 a steady increase of base flow occurs in autumn. The year of 1973 is the wettest year with 1479 mm of precipitation. With stronger variability of both fast flow and base flow caused by numerous rainfall events, its hydrograph differs from the other years.

b. Model specification for this study

Using hourly meteorological data, three model runs covering the period 1 November 1969 to 27 September 1974 are performed

1) using the standard SEWAB version, that is, surface runoff occurs only when the first model layer is saturated and subsurface runoff occurs as free drainage from the lowest model layer (hereinafter SEWAB_STAN);
2) using SEWAB but with VIC model's runoff formulation (hereinafter SEWAB_VIC); and
3) using SEWAB but with TOPMODEL formulations (hereinafter SEWAB_TOP).

The soil and vegetation parameters (Table 1) and the probability distribution function of the topographic index are taken from Stieglitz et al. (1997). The soil column is partitioned into six layers whose thickness increases with depth (0.05, 0.15, 0.26, 0.34, 0.50, and 1.0 m).

c. The snow water equivalent

Seasonal discharge in the W3 subcatchment is dominated by the spring meltwater signal. Therefore, the simulation of the growth and ablation of the snowpack is discussed. Figure 1 shows simulated and measured snow water equivalent (SWE) from November of 1969 to May of 1974. According to Anderson (1976), the error of the measurements is 3%, at least 8 mm yr^{-1} (this does not include errors due to blowing snow). Overall, the growth and ablation of the snowpack for all snow seasons are simulated well. SEWAB strongly underestimates SWE from January of 1970 to the end of the snow season because of two melting events causing outflow that is not observed (see below). The same occurs in the snow season of 1973/74, though here the effect is not that crucial because of a lower total SWE.

In February of 1970, modeled results show a reduction of the SWE from 120 to 84 mm because of melting that is not observed. The meltwater generated by SEWAB left the snowpack, whereas according to the station log the movement of water within the snowpack was considerably delayed. Slush layers existed for several days above ice layers within the snowpack (Anderson 1976). Moreover, Anderson (1976) reports difficulties in the measurement of SWE under such conditions. Measured runoff does show peaks at 3 February, 4 February, and around 12 February (Fig. 3a), indicating error in measuring the snowpack SWE and possible problems with the snow physics.

Altogether, the agreement between measured and simulated SWE is fairly good, although the snow simulation

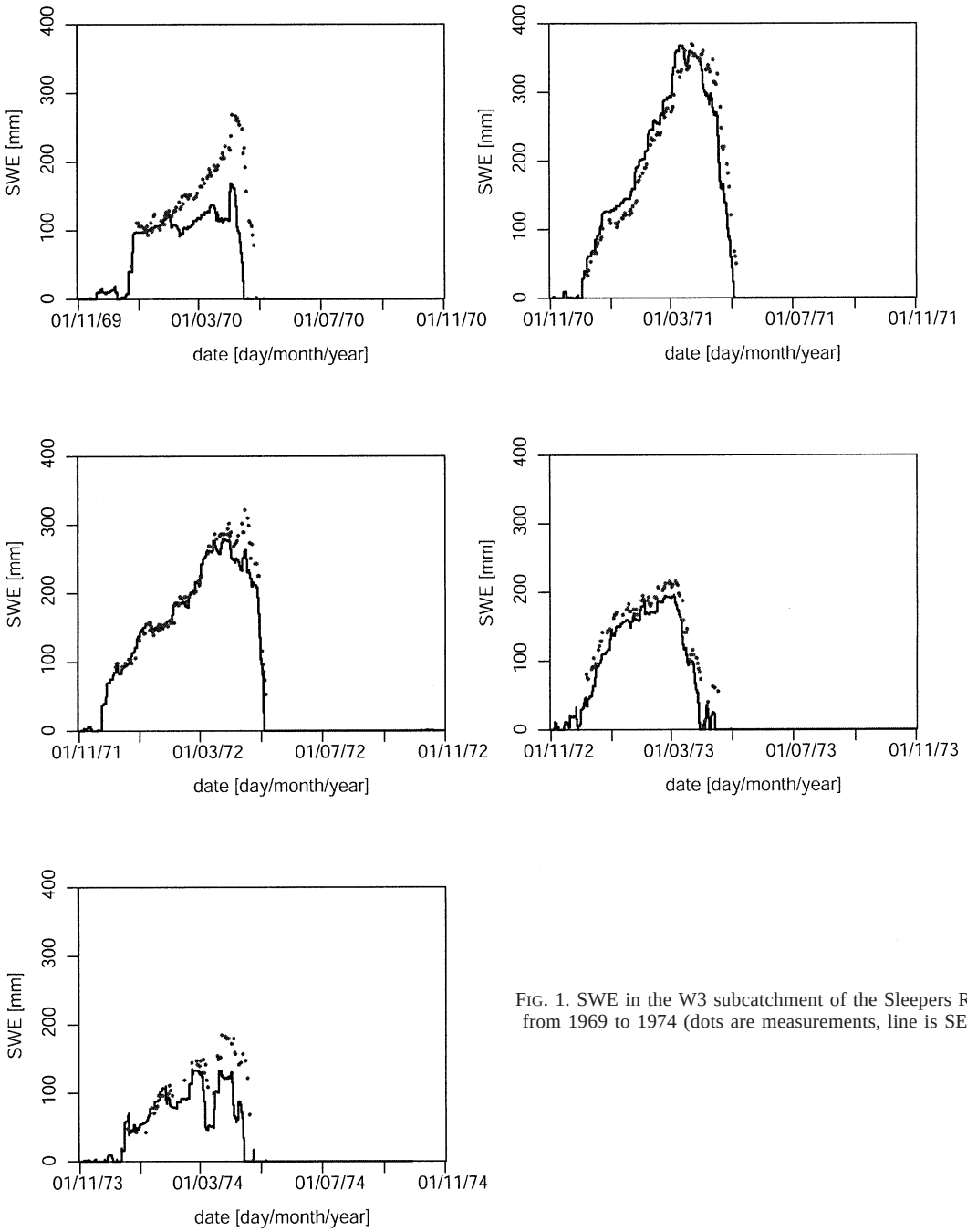

FIG. 1. SWE in the W3 subcatchment of the Sleepers River basin from 1969 to 1974 (dots are measurements, line is SEWAB).

shows differences between measured and simulated SWE and, specifically, an underestimation of SWE. Some of the discrepancies, especially in 1974, may be due to the fact that much of the pack ablation was not due to increase in spring radiation but rather to numerous rain-on-snow events.

d. Runoff

Figures 3–7 compare modeled discharge for SEWAB_STAN, SEWAB_VIC, and SEWAB_TOP with observations. Figure 8 displays the model performance given two criteria of efficiency. Figure 9 shows the annual water balance.

1) CALIBRATION

Following Janssen and Heuberger (1995) quantitative and qualitative criteria were applied for calibration, namely,

1) qualitative agreement between measured and modeled runoff throughout the year,

TABLE 1. Soil parameters (for silty loam) and vegetation parameters (for 100% grass) for the 3 subcatchment of the Sleepers River (Stieglitz et al. 1997, after Rawls et al. 1982, 1993; Hansen et al. 1983). A larger roughness length is observed because trees grow in the neighborhood of the snow research station.

Parameter	Value
Porosity ϕ	0.486
Pore size distribution index b	5.89
Bubbling pressure ψ_s (m)	−0.208
Saturated hydraulic conductivity K_s (m s^{-1})	1.9×10^{-6}
Albedo α	0.22
Leaf area index LAI	0.5–3.0
Roughness length z_0 (m)	0.3
Minimal stomatal resistance R_{smin} (s m^{-1})	17
Vegetation fraction vegf	1.0

2) modeling efficiency (ME),
3) correlation coefficient (R), and
4) annual runoff magnitude.

See appendix C [Eqs. (C1) and (C2)] for the formulation of ME and R. Criterion ME quantifies the relative improvement of the model with respect to the mean value of the observation. A positive value is an improvement over the mean. The R is a measure useful to show the agreement of the temporal variability.

SEWAB_VIC requires the calibration of five parameters [see appendix A, Eqs. (A1) and (A4)]. Because of the good agreement between measured and modeled snow water equivalent and between measured and modeled discharge, we chose 1971 as the period for which model-calibrated parameters were determined. The shape parameter β of the variable infiltration capacity determines the strength of the peak runoff (e.g., 1 August, 5 October). The four base flow parameters d_1, d_2, d_3, and W_s are not independent of each other and need to be adjusted together. Note that, for a given root depth, soil depth, and soil type (see Table 1 and section 4b), the parameters W_1^{max} and W_2^{max} are not subject to calibration. Accordingly, the parameters varied during calibration were β, d_1, d_2, d_3, and W_s. The parameter combination for which qualitative (i.e., visual) agreement was achieved throughout the year and for which ME, R, and annual runoff magnitude were best was chosen for the model application. The set of parameter values obtained from calibration is $\beta = 0.2$, $d_1 = 0.000\ 46$ day^{-1}, $d_2 = 0.003\ 65$ day^{-1}, $d_3 = 2$, and $W_s = 0.46$. Daily runoff is shown in Fig. 4b.

For SEWAB_TOP only decay parameter f is subject to calibration. However, in this study the parameter has been chosen from Stieglitz et al. (1997). SEWAB_STAN has no runoff parameters that require calibration.

2) MODEL APPLICATION FROM 1970 TO 1974

Overall, modeled and measured discharge compare favorably (Figs. 3–7). Depending on the year (1970–74) and the model (SEWAB_STAN, SEWAB_VIC, or SEWAB_TOP), the correlation coefficient ranges between 0.63 and 0.90 (Fig. 8a) and the modeling efficiency varies between 0.26 and 0.81 (Fig. 8b).

(i) Discharge

Runoff simulated with SEWAB_STAN [panel (a) for Figs. 3–7] is relatively unresponsive to both snowmelt generation and precipitation events. For example, in 1971 and 1972, the rise in the snowmelt-related discharge trails the observations by almost two weeks. It seems that the wetting of the soil column needs to be unrealistically high before a discharge response is observed.

Simulations clearly improve by including the VIC-model runoff formulation [SEWAB_VIC; panel (b) for Figs. 3–7]. The quick response to rainfall events agrees with observations in all years. However, because of less water infiltrating into the soil column than in case of SEWAB_STAN, SEWAB_VIC simulates less base flow during the late summer and autumn months. SEWAB_VIC shows an improvement concerning 1) the variability and 2) the runoff due to snowmelt in comparison with SEWAB_STAN.

SEWAB_TOP [panel (c) for Figs. 3–7] shows a further improvement in simulated discharge. Not only is the rise and fall of snowmelt-induced runoff improved in 1971 and 1972, but also the autumn discharge is captured well in 1972 and 1973 and improved in 1971. The variability in the fast runoff is simulated equally well in SEWAB_VIC and SEWAB_TOP; however, SEWAB_TOP better represents both the low-flow period in summer and the system responsiveness in the early autumn.

(ii) Correlation and efficiency

The correlation coefficient R provides a measure of agreement for the temporal variability between observed and simulated runoff (Fig. 8a). Although SEWAB_STAN is relatively unresponsive, it still captures the overall shape of the major discharge event, that is, discharge resulting from the seasonal snowmelt. As such, it yields an R between 0.63 and 0.8, depending on the year. With values between 0.75 and 0.9, SEWAB_VIC and SEWAB_TOP show a considerably larger correlation. In 1973, the correlation of SEWAB_TOP ($R = 0.77$) is only marginally higher than SEWAB_STAN ($R = 0.73$). In 1972 and 1974, SEWAB_TOP's R is 4% and 8%, respectively, higher than SEWAB_VIC's R. The opposite is the case in 1970 (6%) and 1973 (9%). In 1971, for which SEWAB_VIC was calibrated, the R of SEWAB_VIC and SEWAB_TOP are equally good.

The modeling efficiency ME (a measure of the relative improvement of the model with respect to the annual mean value of the observation) is displayed in Fig. 8b. The maximum value of +1 indicates absolute agreement between measured and modeled data. For all the years simulated, each of the three models demonstrates an improvement over the mean. SEWAB_STAN clearly

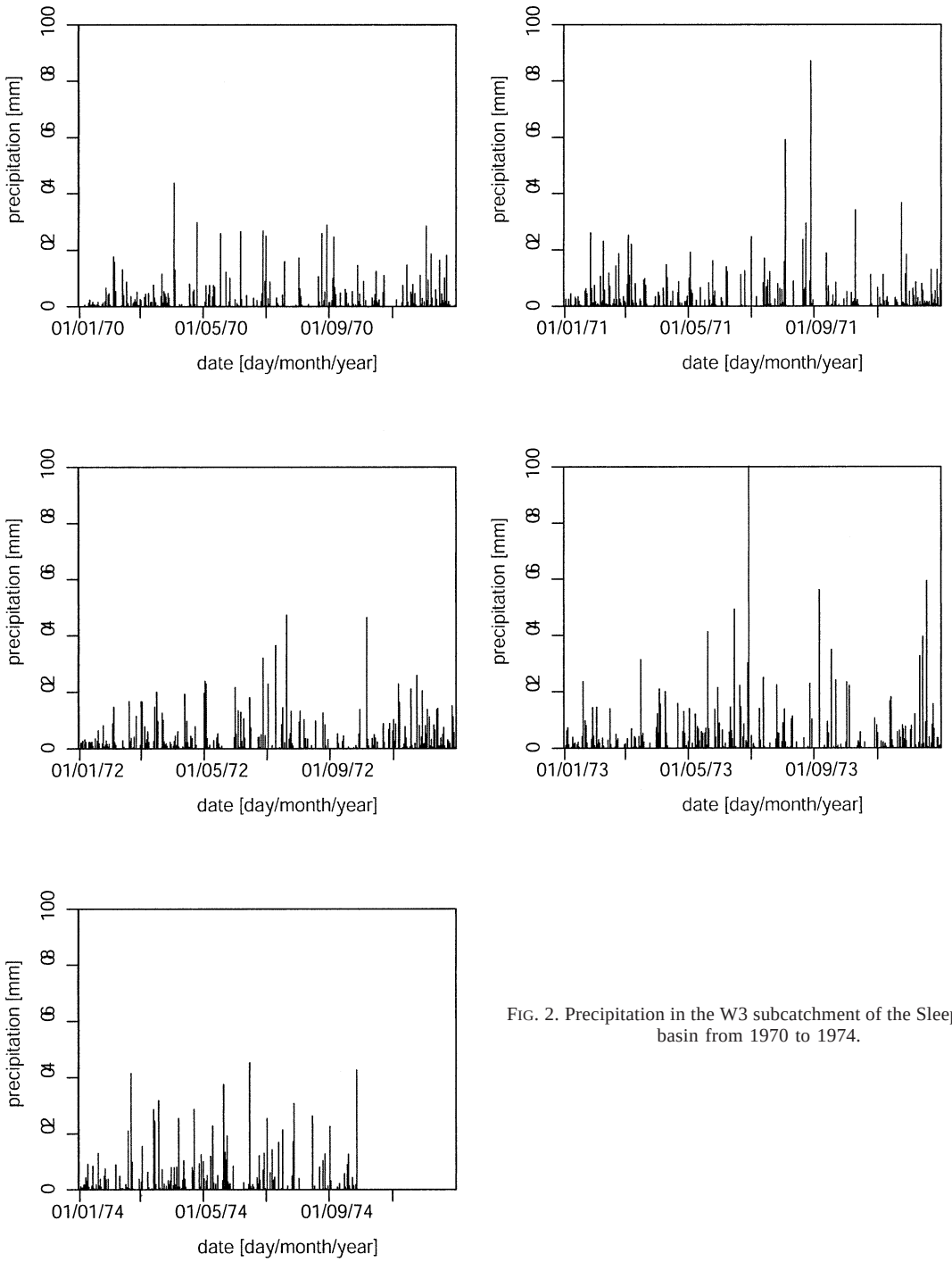

FIG. 2. Precipitation in the W3 subcatchment of the Sleepers River basin from 1970 to 1974.

performs the worst, with ME ranging between 0.26 and 0.54. Overall, both SEWAB_VIC and SEWAB_TOP perform far better than SEWAB_STAN; ME ranges between for 0.47 and 0.75 for SEWAB_VIC and 0.57 and 0.81 for SEWAB_TOP. In 1970 and 1973 ME is larger using SEWAB_VIC, and in 1971, 1972, and 1974 ME is larger using SEWAB_TOP. This quantitative measure shows there to be no clear advantage of using either SEWAB_VIC or SEWAB_TOP.

(iii) Annual water balance

The mean annual soil moisture storage change should be small in comparison with the precipitation, evapo-

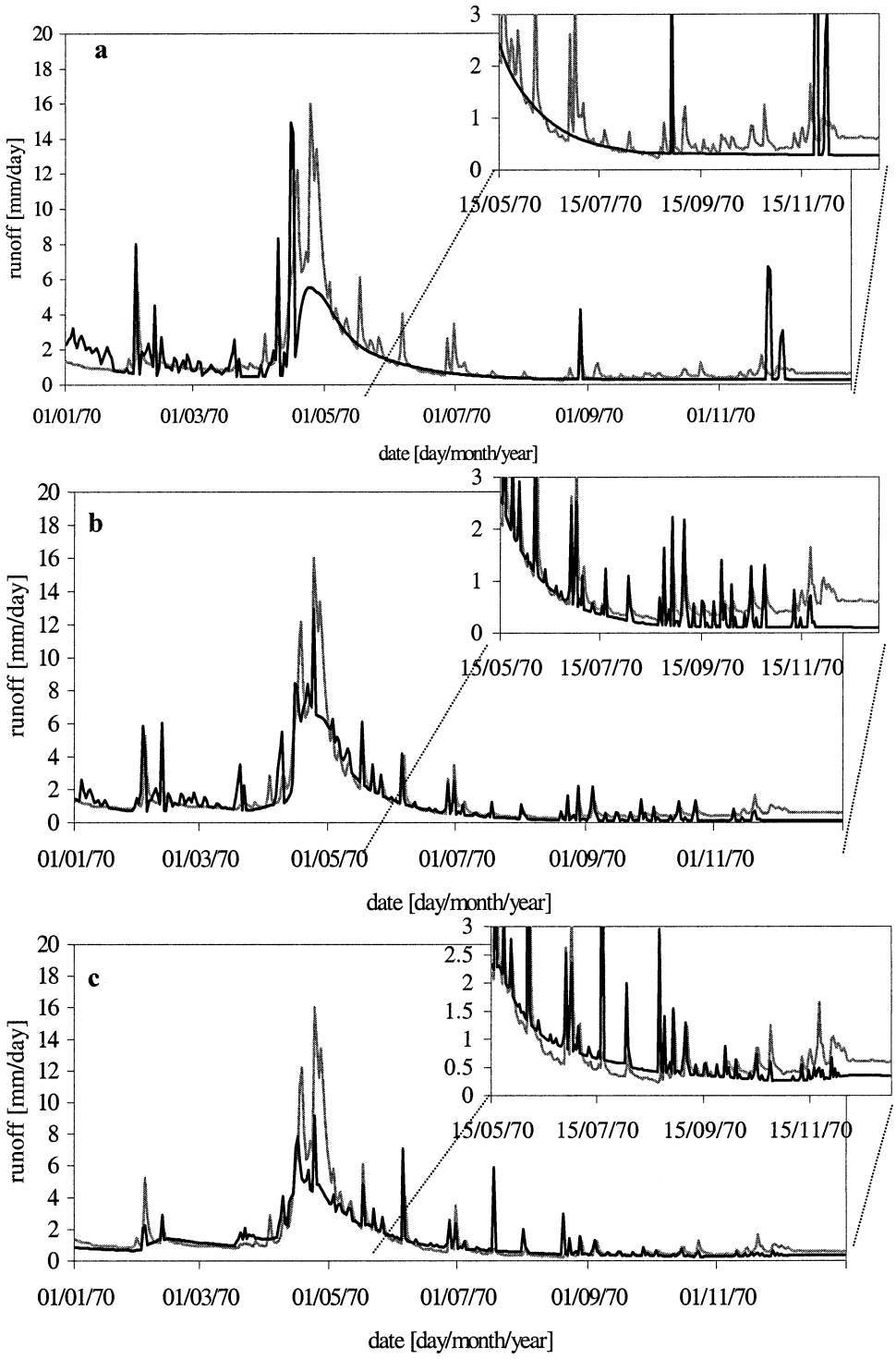

FIG. 3. Measured (gray) and simulated (black) runoff in the W3 subcatchment of the Sleepers River basin from Jan to Dec 1970: (a) SEWAB_STAN, (b) SEWAB_VIC, (c) SEWAB_TOP.

transpiration, and runoff. This is the case for all model simulations. From January 1970 to September 1974, the soil water content of the 2.3-m-deep soil column decreases

1) 79 mm from 729 mm (equivalent to a decrease of soil moisture of 0.03 $m^3\ m^{-3}$) for SEWAB_STAN,
2) 118 mm from 683 mm (equivalent to a decrease of soil moisture of 0.05 $m^3\ m^{-3}$) for SEWAB_VIC, and

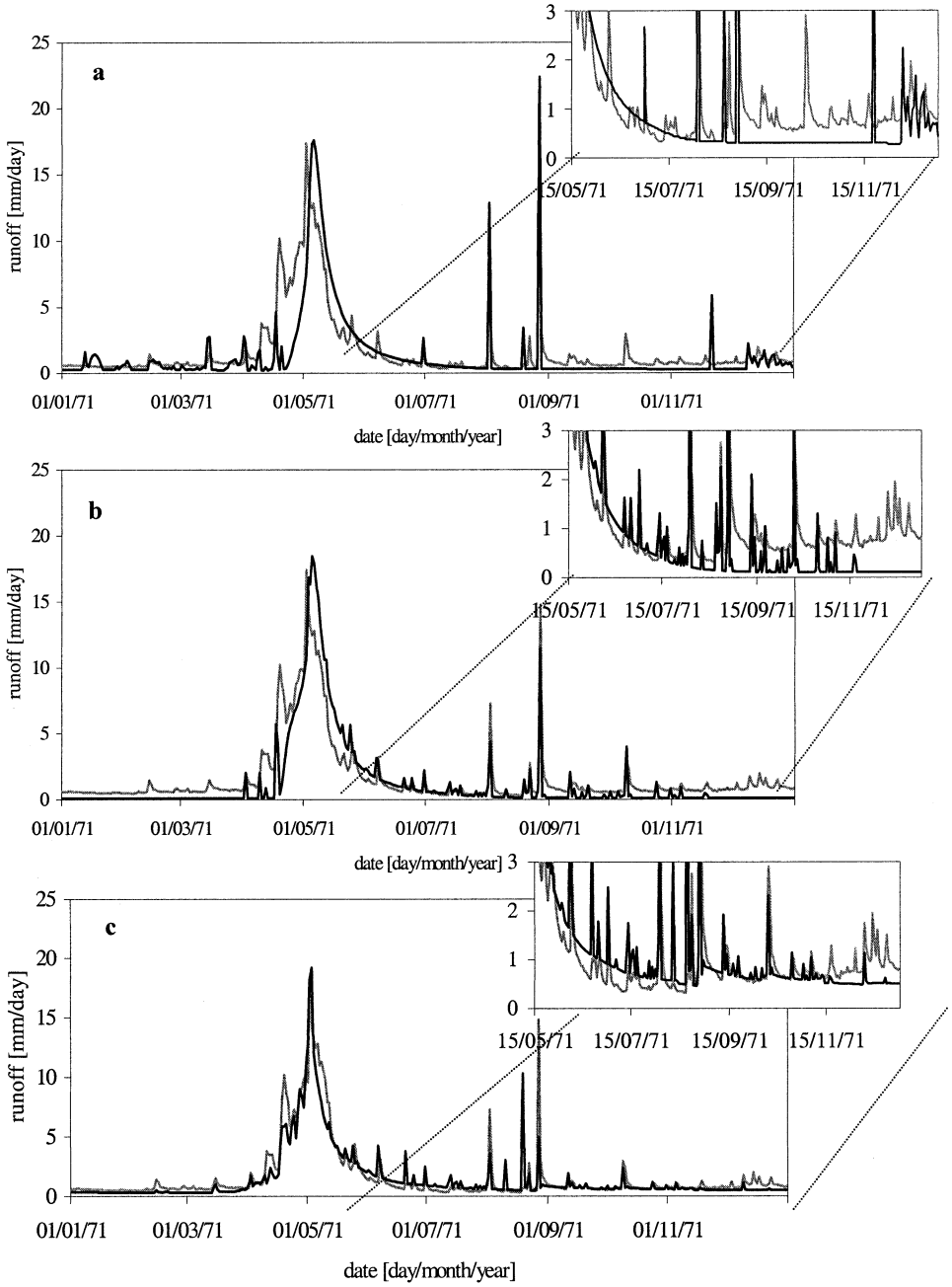

FIG. 4. Same as Fig. 3, but for 1971.

3) 46 mm from 834 mm (equivalent to a decrease of soil moisture of 0.02 $m^3\ m^{-3}$) for SEWAB_TOP.

The simulation is initialized with a soil water content of 690 mm (equivalent to a total soil moisture of 0.3 $m^3\ m^{-3}$) on 1 November 1969. As seen above, the total soil moisture is similar for SEWAB_STAN and SEWAB_VIC but is significantly higher for SEWAB_TOP. The effective saturated hydraulic conductivity in SEWAB_STAN and SEWAB_VIC is constant with depth, but in SEWAB_TOP its exponential decay increases the residence time of water within the soil column with depth. The much higher soil moisture in the case of SEWAB_TOP allows for a wetter and therefore more responsive soil column; that is, less precipitation is needed to lead to runoff production. An additional model simulation with SEWAB_VIC that included SEWAB_TOP's vertical profile of the effective saturated hydraulic conductivity led to a wetter soil column and an improvement of the rising limb of the discharge in

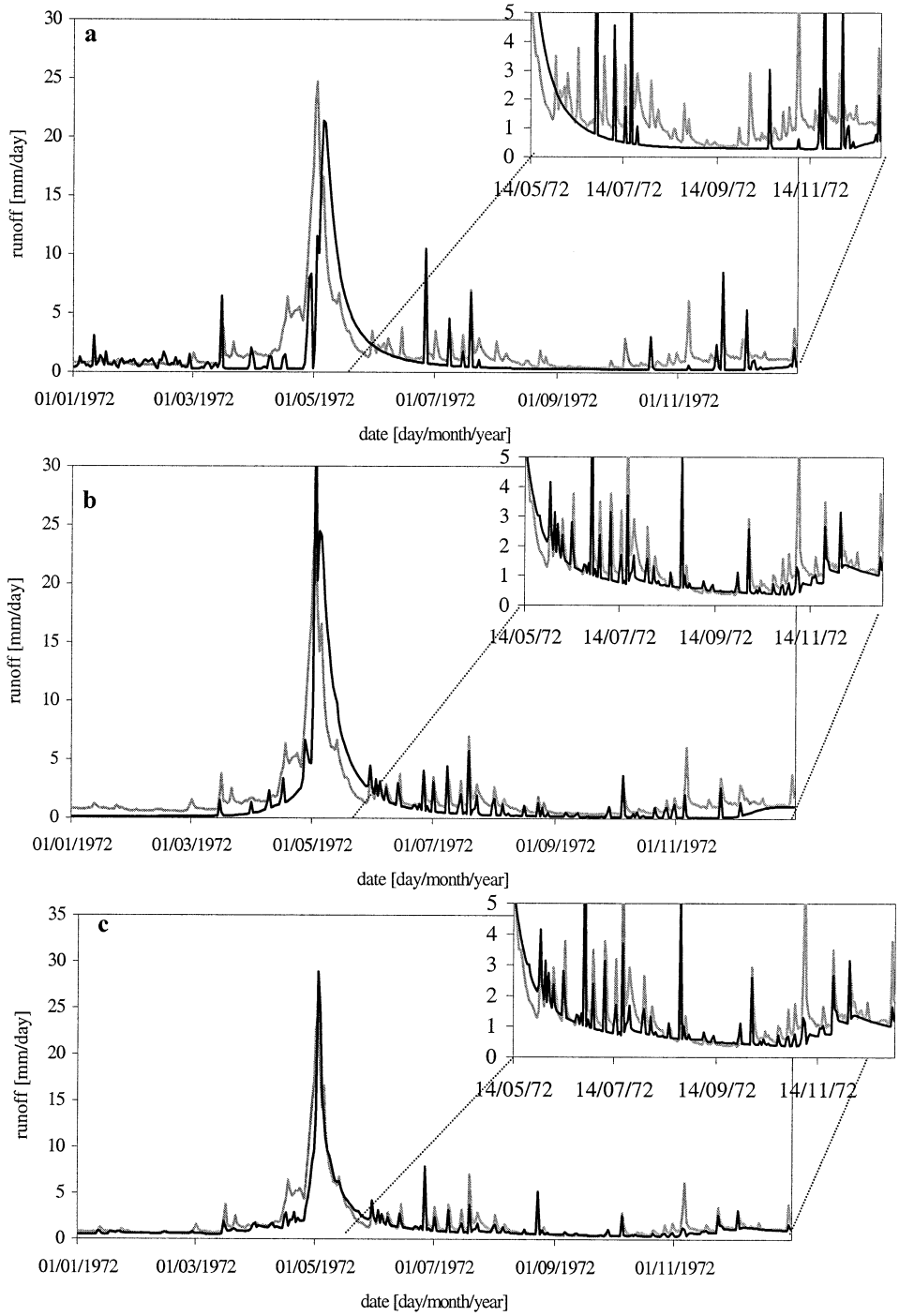

FIG. 5. Same as Fig. 3, but for 1972.

spring and autumn. It did not improve the runoff simulation during the low-flow summer months. (Results are not shown here because this is not a feature of the VIC-model runoff formulation.)

Figure 9 shows the annual precipitation, runoff, evapotranspiration, and runoff deficit from 1970 to 1974. The 1974 data only cover the months from January to September. Over the whole period, the annual mean runoff of 703 mm is underestimated by 10% using SEWAB_TOP, by 16% using SEWAB_VIC, and by 18% using SEWAB_STAN (Fig. 9c). This result is in agreement with the calculations of Stieglitz et al.

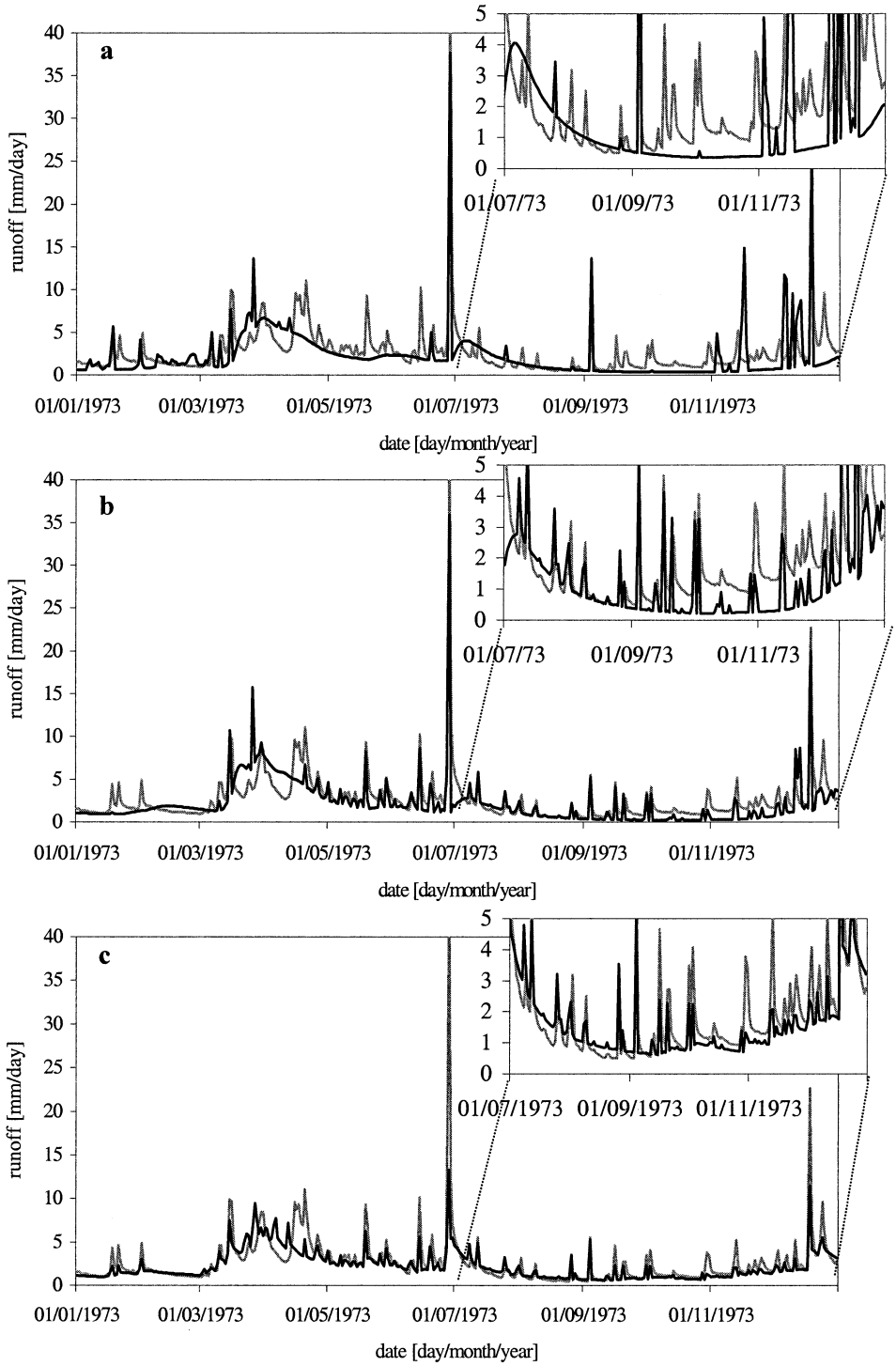

FIG. 6. Same as Fig. 3, but for 1973.

(1997), whose model underestimates the annual mean runoff of the period by 14%. One possible explanation for this is that during high-wind conditions in the winter the measured snow catch is underestimated by about 15% according to Anderson (1976). For the snowfall during the snowmelt season of 1972, Anderson's empirical correction factor for precipitation is 50%, which is in agreement with our findings that yield the greatest modeled underestimation of runoff in 1972 (17%–28% depending on the model).

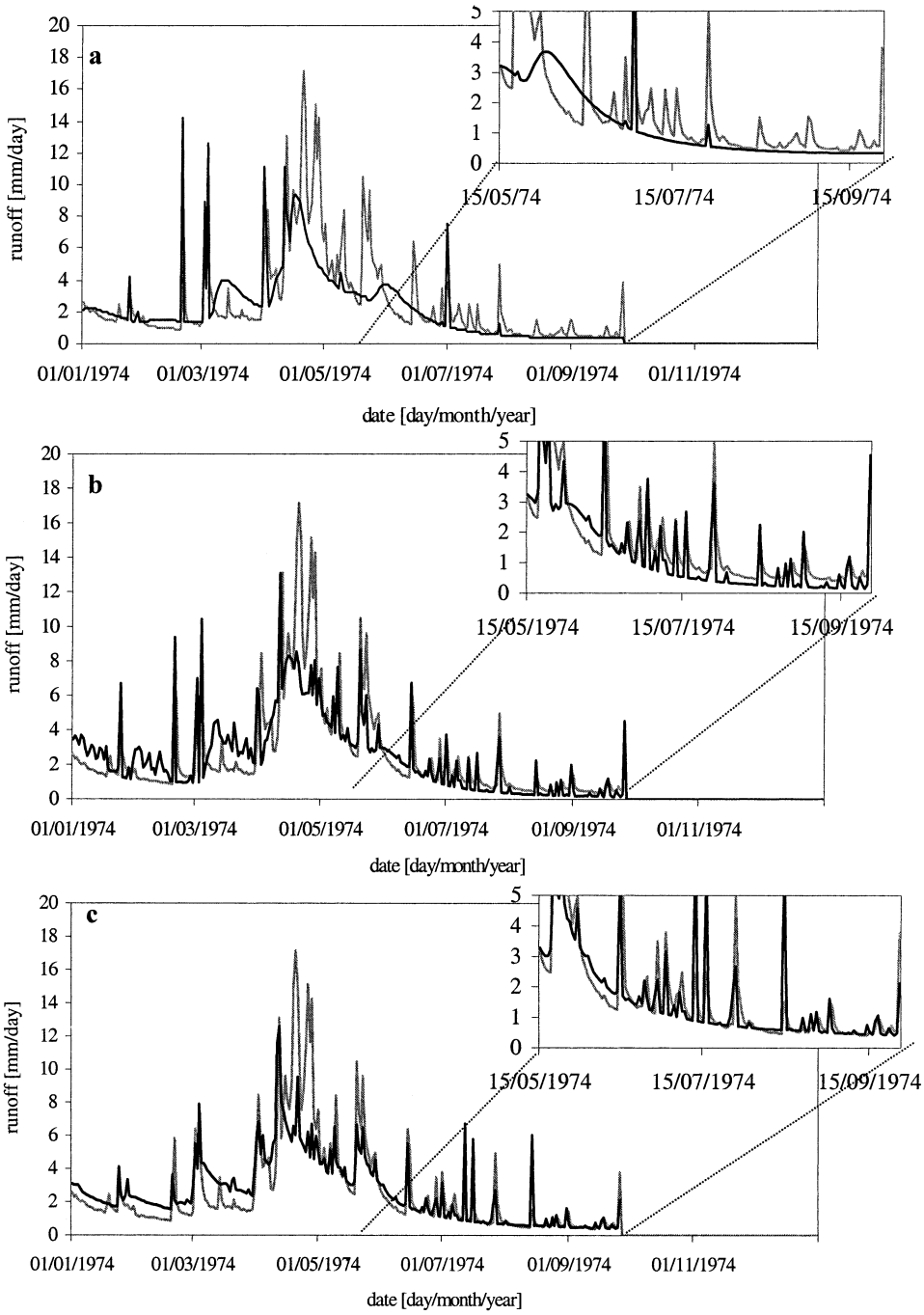

FIG. 7. Same as Fig. 3, but for 1974.

The annual evapotranspiration (Fig. 9b) is almost the same for SEWAB_STAN (mean annual of 590 mm) and SEWAB_VIC (mean annual of 587 mm) but is 10% less for SEWAB_TOP (mean annual of 531 mm). The calculation of the evapotranspiration is the same in all three model versions, but water availability for the evapotranspiration is different. The VIC model takes the saturated and unsaturated fraction of the area into account for runoff generation and bare soil evaporation only. As long as the soil water content within the total root zone is above the wilting point, transpiration occurs. In SEWAB_TOP, transpiration is partitioned between lowland transpiration (in saturated regions) and the upland transpiration. Should the upland soils be below the wilting

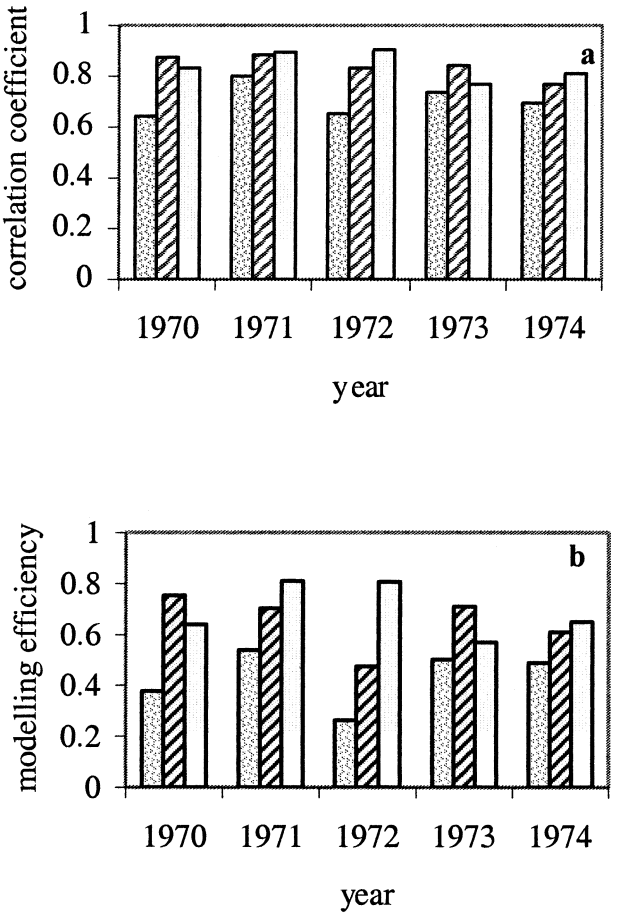

FIG. 8. (a) Correlation coefficient and (b) modeling efficiency for the W3 subcatchment of the Sleepers River basin (SEWAB_STAN dotted, SEWAB_VIC dashed, and SEWAB_TOP filled).

point, upland transpiration will cease while lowland transpiration may continue for some time (until the saturated fraction shrinks to 0).

(iv) Summary

A visual comparison of the daily runoff from January of 1970 to September of 1974 shows a relatively poor simulation when using SEWAB_STAN. The model shows a very damped response to both snowmelt and summer storms. Both hydrological extensions to SEWAB, the VIC-model equations and TOPMODEL equations, led to a significant improvement that is underscored by the correlation coefficients and modeling efficiency values for SEWAB_VIC and SEWAB_TOP. Both VIC and TOPMODEL equations permit for variable infiltration, and therefore, yield ''fast surface'' runoff prior to the complete saturation of the soil. However, because of the vertically decreasing saturated hydraulic conductivity and the manner in which SEWAB_TOP partitions upland and lowland transpiration, SEWAB_TOP retains more soil water than does SEWAB_VIC. As such, it yields a better representation of summertime low-flow conditions and is more responsive to the wetting up of the soil column in the early autumn. For SEWAB_VIC, five base-flow parameters were calibrated for the catchment. For SEWAB_TOP, the topographic index data and the parameter f are taken from Stieglitz et al. (1997). Unlike SEWAB_STAN, both SEWAB_VIC and SEWAB_TOP capture the control that topography has over subgrid soil moisture variability. SEWAB_VIC employs calibrated parameters to capture this topographic control over hydrologic processes, and SEWAB_TOP employs the statistics of site-specific topography.

5. Discussion

We compare three modeling strategies to simulate discharge in a small New England watershed characterized by rolling hills and substantial snow cover. The watershed was chosen because of its excellent hydrometeorological datasets and its location in a hilly midlatitude temperate forest. Most differences between the model strategies show up during the period that is not effected by the snowmelt, that is, the summer and autumn months. This is a ''dry'' period characterized by frequent and heavy rainfall events. Those strategies that attempt to account for spatial heterogeneity in soil moisture (SEWAB_VIC and SEWAB_TOP) yield the best results. SEWAB_TOP, with the highest climatic soil moisture values, performs best during the low-flow conditions and during the autumn wetting up. The wetter years (1973, 1974) yield the least differences in simulated runoff between SEWAB_VIC and SEWAB_TOP.

The improvement using the VIC-model runoff formulation in an SVAT comes with a substantial cost—the addition of five free parameters that must be calibrated for each watershed under consideration. This cost may be prohibitive as modeling moves from simulation at local catchments to regional and global climate studies for which the number a catchments may be thousands and computational expense is at a premium. TOPMODEL, apart from the better capability to simulate runoff during low-flow periods, has the additional advantage that only one tuning parameter (decay factor f) is necessary. However, to account for the effect of the heterogeneity of the topography of the land surface on runoff and saturated fraction, it requires high-resolution elevation data to gain the statistical distribution of the topographic index for a land surface segment.

The variable infiltration capacity and ARNO base flow have been applied successfully on the regional and global scale of GCMs (e.g., Liang et al. 1994; Lohmann et al. 1998a; Hagemann and Dümenil 1999). Lohmann et al.'s (1998c) application of the VIC-2L (two layer) model in the 37 495 km^2 Weser basin (Germany) shows a good agreement of measured and simulated daily streamflow data. Habets et al. (1999) applied the VIC-model runoff formulation in the macroscale ISBA-

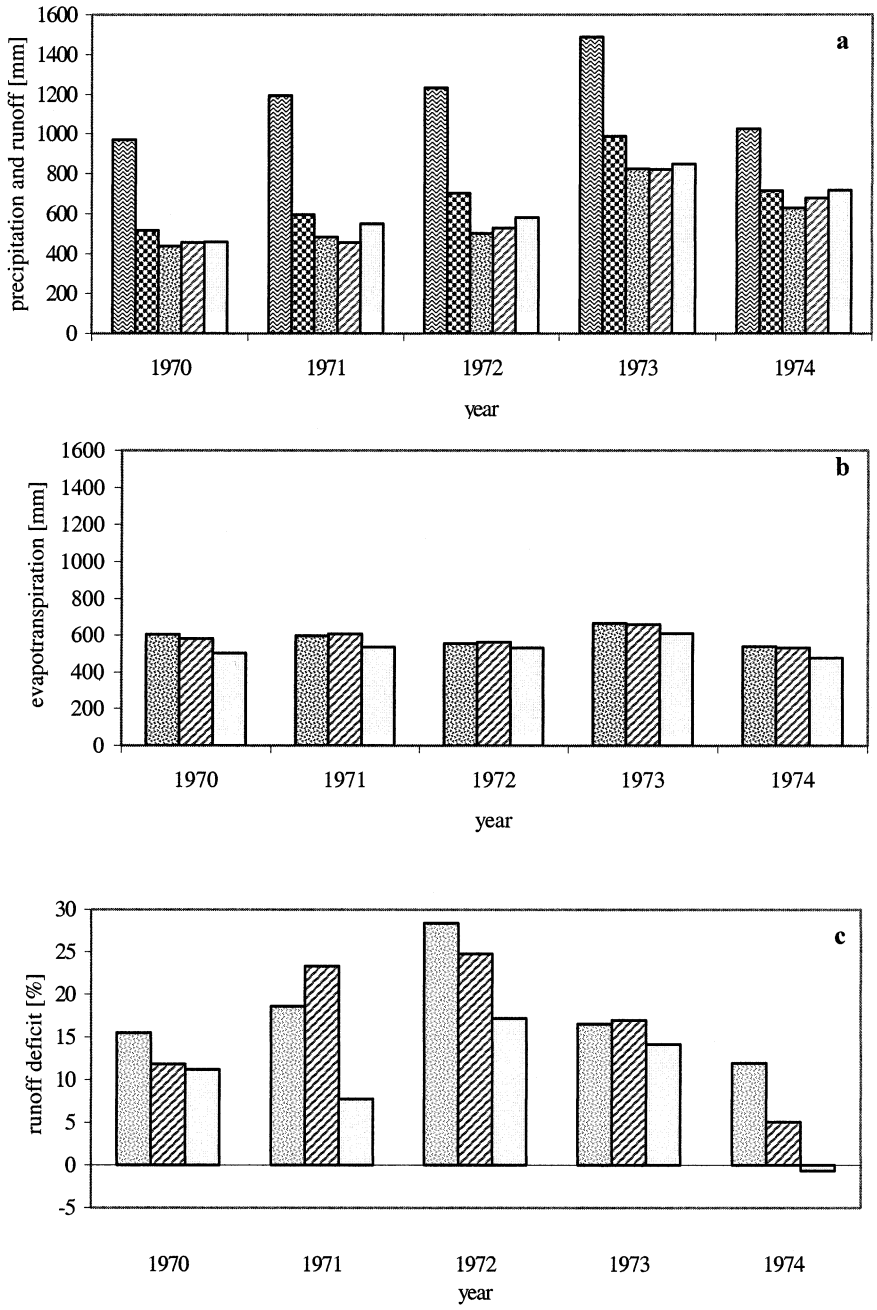

FIG. 9. Annual (a) precipitation and measured and simulated runoff, (b) simulated evapotranspiration, and (c) runoff deficit, i.e., error of simulated runoff in the W3 subcatchment of the Sleepers River basin [precipitation (waves), measured runoff (squares), SEWAB_STAN (dotted), SEWAB_VIC (dashed), SEWAB_TOP (filled)].

MODCOU (coupled model) hydrological model for the Rhone basin (France) on the regional scale with modeling efficiencies between 0.6 and 1.0. For the application to the basin of 86 496 km^2, the SVAT ISBA was applied with the VIC-model runoff formulation on grid cells of 64 km^2. The calculated runoff then was fed into the MODCOU hydrological model (gridcell spacing of 1–8 km), which computes the evolution of the water table, the relation between the water table and the rivers, and the riverflows based on the topography.

In the meantime, Koster et al. (2000) published results demonstrating the progress made by implementing the TOPMODEL concept into LSMs. Their approach also represents a departure from typical LSM modeling in that natural catchment boundaries are used rather than a square grid cell. They discuss the advantages of such

an approach in coupling the LSMs with atmospheric and hydrologic models. Ducharne et al. (2000) performed studies with such an approach for the Arkansas–Red River basin of 600 000 km^2 and show its appropriateness. The only limiting factor in application of this approach is the requirement of high-resolution digital elevation data. This limitation should be overcome in the near future, though. By about two years from now, a global dataset of the topography will be available at a horizontal resolution of 30–90 m from the Shuttle Radar Topography Mission. Until then, one has to rely on scaling techniques as they are described in Ducharne et al. (2000) and Wolock and Price (1994).

Acknowledgments. We thank Dave Wolock for supplying the topographic statistics for the Sleepers River watershed. We also thank E. Anderson at the National Weather Service Hydrologic Research Laboratory, T. Pangburm at the Cold Regions Research and Engineering Laboratory, and J. Thurman at the USDA-ARS Hydrology Laboratory for providing the data of the Sleepers River watershed.

APPENDIX A

Runoff Formulation of the VIC Model

The variable infiltration capacity model is an LSM described in detail by Wood et al. (1992), Liang et al. (1994, 1996), and Lohmann et al. (1998b). The surface runoff (direct runoff) calculation is based on the structure of the Xinanjiang model (Zhao 1992; Zhao and Liu 1995), and subsurface runoff (base flow) follows the ARNO model (Todini 1996).

The VIC model is divided into two (VIC-2L) or three (VIC-3L) vertical soil layers. For simplicity the two-layer version is described (in VIC-3L, the root zone is divided into a thinner top layer and a thicker second layer, and, for the runoff formulation, the second layer of VIC-2L is the third layer in VIC-3L). The VIC model assumes a distribution of local total storage capacities within an area to represent the heterogeneity of the topography, soil type, and vegetation. Rainfall and meltwater fill the storage capacities. Depending on the antecedent soil moisture prior to a precipitation event and the amount of precipitation falling, a fraction A of the land surface is assumed to be saturated, that is, some local storage capacities are filled. This allows surface runoff to be generated without the need for the entire land surface to be saturated. In between rainfall events, the storages drain gravitationally. The so-called variable infiltration capacity form is distributed nonuniformly in space according to

$$I_c = I_{\max}[1 - (1 - A)^{1/\beta}], \qquad 0 \le A \le 1, \quad \text{(A1)}$$

where I_c (m) is the infiltration storage capacity, A is the fraction of the area with infiltration capacity less than I_c, and β is a nondimensional shape parameter that is determined using site discharge measurements; Wood et al. (1992) give its range between 0.1 and 5.0. Here, $I_{\max}$ (m) is the maximum infiltration storage capacity:

$$I_{\max} = W_1^{\max}(1 - \beta), \quad \text{(A2)}$$

where $W_1^{\max}$ (m) is the amount of water in the top soil layer at saturation. The amount of surface runoff R_{surf} (m) during a time step is

$$R_{\text{surf}} = \begin{cases} P + W_1 - W_1^{\max} \\ \quad \forall\ I_0 + P \ge I_{\max} \\ P + W_1 - W_1^{\max}\left[1 - \left(1 - \dfrac{I_0 + P}{I_{\max}}\right)^{1+\beta}\right] \\ \quad \forall\ I_0 + P < I_{\max}, \end{cases} \quad \text{(A3)}$$

where P (m) is the amount of precipitation falling, I_0 (m) is the infiltration capacity at the beginning of the precipitation event, and W_1 (m) is the actual amount of water in the top soil compartment. Note that the VIC approach does not use topographic information; it accounts for the topographic control over surface infiltration implicitly through the shape parameter β.

During the time step Δt (s) the deepest soil layer produces the amount of base flow R_{base} (m) as a nonlinear recession following the Arno model and can be reformulated as

$$R_{\text{base}} = \begin{cases} d_1 W_2 \Delta t \quad \forall\ W_2 \le W_s W_2^{\max} \\ [d_1 W_2 + d_2 (W_2 - W_s W_2^{\max})^{d_3}]\Delta t \\ \qquad \forall\ W_2 > W_s W_2^{\max} \end{cases} \quad \text{(A4)}$$

(Lohmann et al. 1998b), where W_2 (m) is the actual amount of water in the deepest soil layer, $W_2^{\max}$ (m) is W_2 at saturation, W_s is the fraction of $W_2^{\max}$ at which the base flow becomes nonlinear, d_1 (s^{-1}) is the storage constant in the linear storage-outflow region, $(\ln 2)/d_1$ is the half-life decay of the layer, d_2 is the storage coefficient for the nonlinear part of the base-flow recession, and d_3 determines whether this relation itself becomes nonlinear.

The runoff formulation of the VIC model requires the calibration of the parameters β, $W_1^{\max}$, $W_2^{\max}$, d_1, d_2, d_3, and W_s using discharge measurements of the area. Note that in case of a given total soil depth and soil type, $W_1^{\max}$ and $W_2^{\max}$ are not independent of each other. In cases for which root depth and total soil depth are specified in the input dataset, $W_1^{\max}$ and $W_2^{\max}$ are not adjustable parameters.

APPENDIX B

TOPMODEL-Based Runoff Calculation for an SVAT Model

TOPMODEL is a rainfall–runoff model developed by Beven and Kirkby (1979). This approach enables the consideration of the topographic control over the sat-

urated fraction of a watershed and on the surface and subsurface runoff production. Famiglietti and Wood (1994) proposed to represent the moisture distribution within an LSM and the resulting runoff production with a TOPMODEL approach. Following this, Stieglitz et al. (1997) modified the standard TOPMODEL approach by coupling the analytical form of the TOPMODEL equations with a GCM LSM. Because the TOPMODEL approach requires only the statistical distribution of the topography, rather than an explicit accounting of the topography, it can be applied easily at large spatial scales. A summary of this TOPMODEL-based approach of Stieglitz et al. (1997) is given below.

The saturated fraction of a watershed and the resulting base flow can be calculated with the TOPMODEL equations. This approach is based on the following assumptions.

1) The groundwater table is nearly parallel to the soil surface so that the local hydraulic gradient is approximately $\tan\beta$, where β (rad) is the local hill slope angle.
2) The saturated hydraulic conductivity K_s (m s^{-1}), decreases exponentially with depth z (m; positive downward):

$$K_s(z) = K_s(z = 0)\exp(-fz), \tag{B1}$$

   where f is the decay factor of K_s.
3) The groundwater table is recharged at a spatially uniform and steady rate with respect to the response timescale of the watershed. As such, groundwater recharge and base flow are balanced in a series of steady states.

As a result of these approximations an analytical solution exists for the relation between the mean groundwater table depth, $\overline{z}$ (m) and the local groundwater table depth z_x (m) at the location x in the watershed. This can be approximated as

$$z_\chi = \overline{z} - f^{-1}[\ln(a/\tan\beta)_\chi - \Lambda]. \tag{B2}$$

The term $\ln(a\ \tan\beta)_\chi$ is defined to be the topographic index χ, the ratio of the upslope drainage area a to the local slope at that point, $\tan\beta$. The mean watershed value of $\ln(a\ \tan\beta)$ is Λ, and the rate of decline of the saturated hydraulic conductivity is described by f. An immediate consequence of Eq. (B2) can be seen by setting z_χ equal to 0, that is, locating the local water table depth at the surface. All locations associated with values of the topographic index χ greater than $\Lambda + f\overline{z}$ are situated within saturated regions. Last, following Sivapalan et al. (1987), the base flow R_b (m s^{-1}) can be calculated by integrating Eq. (B2) along the river network of the watershed:

$$R_b = \frac{K_s(z = 0)}{f}\exp(-\Lambda)\exp(-f\overline{z}). \tag{B3}$$

Therefore, from knowledge of the mean groundwater table depth and the cumulative distribution of the topographic index, which is gained from DEM data, the saturated fraction f_{sat} of the watershed and the corresponding base flow can be calculated. For a complete description of the model, see Beven and Kirkby (1979) and Beven (1986 a,b).

To reduce the computational expense for large-scale applications, Stieglitz et al. (1997) coupled the analytical form of the TOPMODEL equations with a standard (one dimensional) soil column LSM. The ground scheme consists of 10 soil layers. Diffusion and a modified tipping-bucket model govern heat and water flow, respectively. The prognostic variables, heat and water content, are updated at each time step. In turn, the fraction of ice and temperature of a layer may be determined from these variables. Transpiration and other surface energy balance calculations use a standard vegetation model that includes bare-soil evaporation and canopy interception loss. At each time step, the mean water table is updated. TOPMODEL equations and DEM data then are used to generate base flow R_b, which supports the lowland saturated areas. Soil moisture heterogeneity represented by saturated lowlands (predicted by TOPMODEL equations) subsequently impacts watershed evapotranspiration, the partitioning of surface fluxes, and the development of the storm hydrograph. Evapotranspiration, surface runoff, and heat fluxes are calculated separately for the saturated and unsaturated fraction and are averaged for the segment.

The variables $\overline{z}$, f_{sat}, and R_b are calculated as follows. Searching from the bottom of the soil profile, the mean groundwater table is located to be within the first unsaturated soil layer i such that

$$\overline{z} = \mathrm{zb}_i \qquad \forall\ \eta_i < 0.7\eta_{fc}, \tag{B4}$$

and

$$\overline{z} = \mathrm{zb}_i - \left(\frac{\eta_i - 0.7\eta_{fc}}{\phi - 0.7\eta_{fc}}\right)\Delta z_i \quad \forall\ \eta_i > 0.7\eta_{fc}, \tag{B5}$$

where zb_i (m) is the depth of lower boundary for layer i, ϕ is the porosity, η_{fc} is the soil moisture at field capacity, and η_i is the soil moisture of layer i. The saturated fraction f_{sat} is then calculated as the area under the cumulative distribution of the topographic index with $\chi > \Lambda + f\overline{z}$; R_b is determined from Eq. (B2). Both f_{sat} and R_b vanish if the lowest model layer is unsaturated. SEWAB is applied in its standard version (Mengelkamp et al. 1999) to calculate vertical water fluxes for the unsaturated fraction of the land surface.

If the mean groundwater table is located in soil layer $i = j$, the base flow is distributed among the soil layers i as follows:

$$R_{b,j} = \left[\frac{K_{s,j}(\mathrm{zb}_j - \overline{z})}{K_{s,j}(\mathrm{zb}_j - \overline{z}) + \sum_{i=j+1}^{n} K_{s,i}\Delta z_i}\right]R_b \quad \text{and} \tag{B6}$$

$$R_{b,i} = \left[\frac{K_{s,i}\Delta z_i}{K_{s,j}(\mathrm{zb}_j - \bar{z}) + \sum_{i=j+1}^{n} K_{s,i}\Delta z_i}\right] R_b$$

$$\forall\ j + 1 \le i \le n, \qquad \text{(B7)}$$

where n denotes the lowest soil layer. Because of the exponential decay of the saturated hydraulic conductivity, the residence time of water within the soil column increases with depth.

APPENDIX C

Performance Measures for Comparison of Modeled and Measured Data

Janssen and Heuberger (1995) summarize a variety of measures to compare model predictions with observations quantitatively. The following measures are used here: modeling efficiency (ME; in hydrology also known as Nash–Sutcliffe coefficient),

$$\mathrm{ME} = \frac{\left[\sum_{i=1}^{N} (O_i - \overline{O})^2 - \sum_{i=1}^{N} (S_i - O_i)^2\right]}{\left[\sum_{i=1}^{N} (O_i - \overline{O})^2\right]}, \quad \text{and} \qquad \text{(C1)}$$

correlation coefficient R,

$$R = \frac{\sum_{i=1}^{N} (S_i O_i) - \frac{1}{N}\sum_{i=1}^{N} S_i \sum_{i=1}^{N} O_i}{\sqrt{\left[\sum_{i=1}^{N} (S_i)^2 - \frac{1}{N}\left(\sum_{i=1}^{N} S_i\right)^2\right]\left[\sum_{i=1}^{N} (O_i)^2 - \frac{1}{N}\left(\sum_{i=1}^{N} O_i\right)^2\right]}}, \qquad \text{(C2)}$$

where N is the number of data, that is, in this case, 365 and 366 days, respectively; O_i and S_i denote the observed and simulated value at i, and $\overline{O}$ is the observed mean annual values. In this study, O_i and S_i denote the observed and simulated runoff at day i, and $\overline{O}$ is the observed mean annual runoff. The closer ME and R are to $+1$ the better the simulation is.

REFERENCES

Abdullah, F. A., D. P. Lettenmaier, E. F. Wood, and J. A. Smith, 1996: Application of a macroscale hydrologic model to estimate the water balance of the Arkansas–Red River basin. *J. Geophys. Res.,* **101,** 7449–7459.

Anderson, E. A., 1976: A point energy mass balance model for a snow cover. NOAA Tech. Rep. NWS 19, 150 pp.

Beven, K. J., 1986a: Hillslope runoff processes and flood frequency characteristics. *Hillslope Processes,* A. D. Abrahams, Ed., Allan and Unwin, 187–202.

——, 1986b: Runoff production and flood frequency in catchments of order *n*: An alternative approach. *Scale Problems in Hydrology,* V. K. Gupta, I. Rodriguez-Iturbe, and E. F. Wood, Eds., D. Reidel, 107–131.

——, 2000: *Rainfall–Runoff Modelling: The Primer*. John Wiley and Sons, 360 pp.

——, and M. J. Kirkby, 1979: A physically-based variable contributing area model of basin hydrology. *Hydrol. Sci. J.,* **24,** 43–69.

Bonan, G. B., 1995: Land–atmosphere CO_2 exchange simulated by a land surface process model coupled to an atmospheric general circulation model. *J. Geophys. Res.,* **100,** 2817–2831.

Chen, F., and Coauthors, 1996: Modeling of land surface evaporation by four schemes and comparison with FIFE observations. *J. Geophys. Res.,* **101,** 7251–7268.

Chen, T. H., and Coauthors, 1997: Cabauw experimental results from the Project for Intercomparison of Land-Surface Parameterization Schemes. *J. Climate,* **10,** 1194–1215.

Ducharne, A., R. D. Koster, M. J. Suarez, M. Stieglitz, and P. Kumar, 2000: A catchment-based approach to modeling land surface processes. Part 2: Parameter estimation and model demonstration. *J. Geophys. Res.,* **105,** 24 823–24 838.

Dümenil, L., and E. Todini, 1992: A rainfall–runoff scheme for use in the Hamburg climate model. *Advances in Theoretical Hydrology, A Tribute to James Dooge,* J. P. O'Kane, Ed., European Geophysical Society Series on Hydrological Sciences Vol. 1, Elsevier, 129–157.

Famiglietti, J. S., and E. F. Wood, 1994: Multiscale modeling of spatially variable water and energy balance processes. *Water Resour. Res.,* **30,** 3061–3078.

Graham, L. P., and S. Bergström, 2000: Land surface modelling in hydrology and meteorology—Lessons learned from the Baltic Basin. *Hydrol. Earth Syst. Sci.,* **4,** 13–22.

Habets, F., P. Etchevers, C. Golaz, E. Leblois, E. Ledoux, E. Martin, J. Noilhan, and C. Ottlé, 1999: Simulation of the water budget and the river flows of the Rhone basin. *J. Geophys. Res.,* **104,** 31 145–31 172.

Hagemann, S., and L. Dümenil, 1999: Application of a global discharge model to atmospheric model simulations in the BALTEX region. *Nordic Hydrol.,* **30,** 209–230.

Hansen, J. E., G. Russel, D. Rind, P. H. Stone, A. A. Lacis, S. Lebedeff, R. Ruedy, and L. Travis, 1983: Efficient three-dimensional global models for climate studies: Models I and II. *Mon. Wea. Rev.,* **111,** 609–662.

Henderson-Sellers, A., Z.-L. Yang, and R. E. Dickinson, 1993: The Project for Intercomparison of Land-Surface Parameterization Schemes. *Bull. Amer. Meteor. Soc.,* **74,** 1335–1349.

Janssen, P. H. M., and P. S. C. Heuberger, 1995: Calibration of process-oriented models. *Ecol. Modell.,* **83,** 55–66.

Koster, R. D., M. J. Suarez, A. Ducharne, M. Stieglitz, and P. Kumar, 2000: A catchment-based approach to modeling land surface processes in a GCM. Part 1: Model structure. *J. Geophys. Res.,* **105,** 24 809–24 822.

Kucharik, C. J., and Coauthors, 2000. Testing the performance of a dynamic global ecosystem model: Water balance, carbon balance, and vegetation structure. *Global Biogeochem. Cycles,* **14,** 795–825.

Liang, X., D. P. Lettenmaier, E. F. Wood, and S. J. Burges, 1994: A simple hydrologically based model of land surface water and energy fluxes for general circulation models. *J. Geophys. Res.,* **99,** 14 415–14 428.

——, E. F. Wood, and D. P. Lettenmaier, 1996: Surface soil moisture parameterization of the VIC-2L model: Evaluation and modification. *Global Planet. Change,* **13,** 195–206.

Lohmann, D., and Coauthors, 1998a: The Project for Intercomparison of Land-surface Parameterization Schemes (PILPS) Phase2(c) Red–Arkansas River Basin Experiment: 3. Spatial and temporal analysis of water fluxes. *Global Planet. Change,* **19,** 161–179.

——, E. Raschke, B. Nijssen, and D. P. Lettenmaier, 1998b: Regional scale hydrology: I. Formulation of the VIC-2L model coupled to a routing model. *Hydrol. Sci.,* **43,** 131–142.

——, ——, ——, and ——, 1998c: Regional scale hydrology: II. Application of the VIC-2L model to the Weser River, Germany. *Hydrol. Sci.,* **43,** 143–158.

Mengelkamp, H.-T., K. Warrach, and E. Raschke, 1999: SEWAB: A parameterization of the surface energy and water balance for atmospheric and hydrologic models. *Adv. Water Res.*, **23,** 165–175.

Nijssen, B., R. Schnur, and D. P. Lettenmaier, 2001: Global retrospective estimation of soil moisture using the Variable Infiltration Capacity land surface model, 1980–93. *J. Climate,* **14,** 1790–1808.

Noilhan, J., and S. Planton, 1989: A simple parameterization of land surface processes for meteorological models. *Mon. Wea. Rev.*, **117,** 536–549.

Rawls, W. J., D. L. Brakensiek, and K. E. Saxton, 1982: Estimation of soil water properties. *Trans. ASAE,* **25,** 1316–1320.

——, L. R. Ahuja, D. L. Brakensiek, and A. Shirmohammadi, 1993: Infiltration and soil water movement. *Handbook of Hydrology,* D. R. Maidment, Ed., McGraw-Hill, 5.1–5.51.

Richtmyer, R. D., and K. W. Morton, 1967: *Difference Methods for Initial Value Problems.* Wiley Intersciences, 406 pp.

Schulz, J.-P., L. Dümenil, J. Polcher, C. A. Schlosser, and Y. Xue, 1998: Land surface energy and moisture fluxes: Comparing three models. *J. Appl. Meteor.,* **37,** 288–307.

Sellers, P. J., Y. Mintz, Y. C. Sud, and A. Dalcher, 1986: A simple biosphere model (SiB) for use within general circulation models. *J. Atmos. Sci.,* **43,** 505–531.

Sivapalan, M., K. Beven, and E. F. Wood, 1987: On hydrologic similarity. 2. A scaled model of storm runoff production. *Water Resour. Res.,* **23,** 2266–2278.

Slater, A. G., and Coauthors, 2001: The representation of snow in land-surface schemes: Results from PILPS 2(d). *J. Hydrometeor.,* **2,** 7–25.

Stieglitz, M., D. Rind, J. Famiglietti, and C. Rosenzweig, 1997: An efficient approach to modeling the topographic control of surface hydrology for regional and global climate modeling. *J. Climate,* **10,** 118–137.

Todini, E., 1996: The Arno rainfall–runoff model. *J. Hydrol.,* **175,** 339–382.

Verseghy, D. L., N. A. McFarlane, and M. Lazare, 1993: A Canadian land surface scheme for GCMs: II. Vegetation model and coupled runs. *Int. J. Climatol.,* **13,** 347–370.

Warrach, K., H.-T. Mengelkamp, and E. Raschke, 2001: Treatment of frozen soil and snow cover in the land surface model SEWAB. *Theor. Appl. Climatol.,* **69,** 23–37.

Wolock, D. M., and C. V. Price, 1994: Effects of digital elevation model map scale and data resolution on a topography based watershed model. *Water Resour. Res.,* **30,** 3041–3052.

——, and G. J. McCabe, 2000: Differences in topographic characteristics computed from 100- and 1000-meter resolution digital elevation model data. *Hydrol. Processes,* **14,** 987–1002.

Wood, E. F., D. P. Lettenmaier, and V. G. Zartarian, 1992: A land-surface hydrology parameterization with subgrid variability for general circulation models. *J. Geophys. Res.,* **97,** 2717–2728.

——, and Coauthors, 1998: The Project for Intercomparison of Land-Surface Parameterization Schemes (PILPS) Phase2(c) Red–Arkansas River basin experiment: 1. Experiment description and summary intercomparisons. *Global Planet. Change,* **19,** 115–136.

Yang, Z.-L., and R. E. Dickinson, 1996: Description of the Biosphere–Atmosphere Transfer Scheme (BATS) for the soil moisture workshop and evaluation of its performance. *Global Planet. Change,* **13,** 117–134.

Zhang, W., and D. R. Montgomery, 1994: Digital elevation model grid size, landscape representation, and hydrologic simulations. *Water Resour. Res.,* **30,** 1019–1028.

Zhao, R. J., 1992: The Xinanjiang model applied in China. *J. Hydrol.,* **134,** 371–381.

——, and X.-R. Liu, 1995: The Xianjiang model. *Computer Models of Watershed Hydrology,* V. P. Singh, Ed., Water Resources Publications, 215–232.